Single-Molecule Magnets

George Christou, Dante Gatteschi,
David N. Hendrickson, and Roberta Sessoli

Introduction

Magnets are widely used in a large number of applications, and their market is larger than that of semiconductors. Information storage is certainly one of the most important uses of magnets, and the lower limit to the size of the memory elements is provided by the superparamagnetic size, below which information cannot be permanently stored because the magnetization freely fluctuates. This occurs at room temperature for particles in the range of 10–100 nm, owing to the nature of the material. However, even smaller particles can in principle be used either by working at lower temperatures or by taking advantage of the onset of quantum size effects, which can make nanomagnets candidates for the construction of quantum computers.

An important point is that the properties of magnetic particles scale exponentially, and therefore either it must be possible to address individual particles, or ensembles of absolutely identical particles must be available. This has presented a formidable challenge, but an attractive potential solution is provided by the recent realization that molecules containing several transition-metal ions can exhibit properties similar to nanoscale magnetic particles (nanomagnets). For this reason, such polynuclear metal complexes exhibiting superparamagnetic-like properties have been called *single-molecule magnets* (SMMs).[1] An overview of ongoing SMM research is presented in this review, with the goal of describing the factors determining their magnetic properties and giving some indication of possible applications.

Origin of Single-Molecule Magnetism

In 1993, the first SMM, the compound $[Mn_{12}O_{12}(O_2CCH_3)_{16}(H_2O)_4]\cdot 4H_2O\cdot 2CH_3CO_2H$ (Complex **1**), was discovered.[2–4] A drawing of the $Mn_{12}O_{12}$ core of Complex **1** is shown in Figure 1. Variable-field magnetization and high-frequency electron paramagnetic resonance (HFEPR) data indicate that **1** has an $S = 10$ ground state. The large spin ground state arises from antiferromagnetic interactions between the $S = 3/2$ spins of Mn^{IV} ions and the $S = 2$ spins of Mn^{III} ions, which do not compensate. An axial zero-field splitting is present, and this leads to a splitting of the $S = 10$ state into 21 levels, each characterized by a spin projection quantum number, m_s, where $-S \le m_s \le S$. Each level has an energy given as $E(m_s) = m_s^2 D$, where for **1** it has been found that the axial zero-field splitting parameter $D = -0.50$ cm^{-1} ($\equiv -0.70$ K). The negative sign of D leads to a potential-energy barrier between the "spin-up" ($m_s = -10$) and "spin-down" ($m_s = 10$) orientations of the magnetic moment of an individual Mn_{12} molecule (Figure 2). In other words, in order to flip the spin of a Mn_{12} molecule from along the $+z$ axis (Figure 1) to along the $-z$ axis of the disc-like $Mn_{12}O_{12}$ core, it takes some energy (the barrier in Figure 2) to reorient the spin via the perpendicular $m_s = 0$ state. This is an easy axis type of anisotropy. If this barrier is appreciable, the spin of an SMM can be magnetized in one direction. For **1**, the barrier must be $E(m_s = 0) - E(m_s = \pm 10) = 100D \approx 70$ K. For a thermally activated process, the time for the reorientation of the magnetization depends exponentially on the height of the barrier. If **1** is magnetized at 2 K by applying a magnetic field and then removing the field, the relaxation of the magnetization is so slow that after two months the magnetization is still about 40% of the saturation (i.e., largest) value. At 1.5 K, the half-life for magnetization decay is hardly measurable because it is too long. It has been conclusively established that the slow magnetization relaxation shown by an SMM is due to an individual molecule rather than to long-range ordering as observed in nanoscale magnetic domains of bulk magnets. Support for this conclusion comes from several experiments, such as magnetization relaxation data for frozen solutions[5] or polymer-doped samples, the absence of any anomaly in heat-capacity measurements[6] (no long-range magnetic ordering), and high-frequency electron paramagnetic resonance (HFEPR) data.[4]

When a sample of **1** is exposed to a large external magnetic field, the $m_s = -10$ state is greatly stabilized in energy relative to the $m_s = +10$ state. All of the **1** molecules

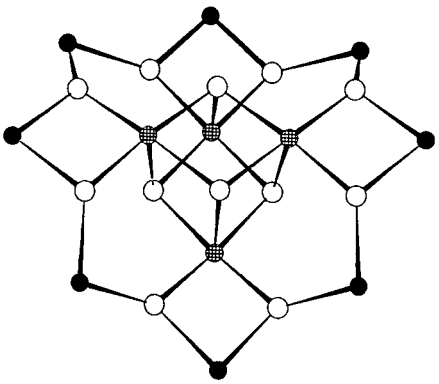

*Figure 1. Drawing of the $[Mn^{IV}_4Mn^{III}_8(\mu\text{-}O)_{12}]^{16+}$ core of $[Mn_{12}O_{12}(O_2CCH_3)_{16}(H_2O)_4]\cdot 4H_2O\cdot 2CH_3CO_2H$ (Complex **1**), showing the relative positions of the Mn^{IV} ions (shaded circles), Mn^{III} ions (solid circles), and μ_3-O^{2-} bridges (open circles).*

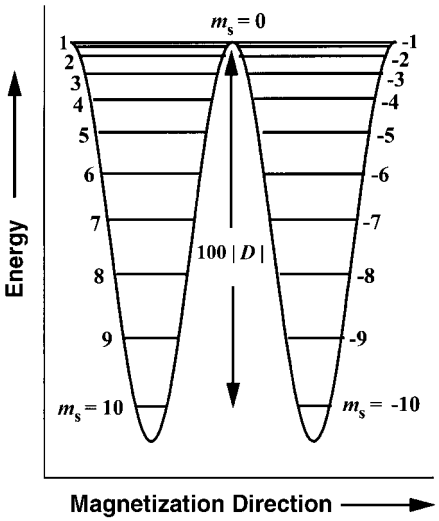

Figure 2. Plot of the potential energy versus the magnetization direction for a single-molecule magnet (SMM) with an $S = 10$ ground state experiencing axial zero-field splitting, $D\hat{S}_z^2$, where $\hat{S}_z$ is the zth component of the electron spin operator. The diagram is for zero external magnetic field.

have their spins aligned with the external field; all of the molecules are in the $m_s = -10$ state, and the magnetization is saturated. If the external field is cycled to zero, the magnetization M is frozen by the presence of the barrier and only very slowly tends to the equilibrium value ($M = 0$). Thus, a remanent magnetization is observed. A negative field reduces the height of the barrier and unfreezes the spins, thus allowing a rapid reversal of the magnetization. A hysteresis loop is therefore observed, which has a molecular and dynamical origin. The width of the loop (i.e., the coercive field) depends on the temperature as well as the rate of sweep of the magnetic field. Large coercive fields of several Tesla have been observed for **1** below 2 K. The important feature is that at zero field, the magnetization of **1** can be either positive or negative, depending on the history of the sample. Therefore, it is possible in principle to store information in one single, bistable molecule.

The magnetic anisotropy of the ground state of **1** largely results from the magnetic anisotropy of the eight Mn^{III} ions. The bonding at each Mn^{III} ion is such that two *trans*- bonds are longer than the other four (in what is called a *Jahn–Teller elongation*). These "crystal-field" distortions, together with a spin-orbit interaction, establish a zero-field splitting at each Mn^{III} ion. Thus, it is the vectorial projection of single-ion anisotropies onto the $S = 10$ ground state that gives rise to the easy axis type of magnetoanisotropy. When the single-ion anisotropy is small, as in some Fe^{III} clusters, the anisotropy originating from dipolar interactions is no longer negligible. In this case, ferrimagnetic planar structures are more suited to give an easy axis magnetoanisotropy.[7]

Synthesis of SMMs

It is clear from the brief introduction just given that several synthesis-design principles exist. The potential-energy barrier scales with essentially the square of the ground-state spin and linearly with the axial zero-field splitting parameter D. It is desirable to prepare SMMs with larger and larger S values and with appreciable negative D values. Polynuclear metal complexes containing Mn, Fe, V, or Cr have been shown to function as SMMs.

The preparation of polynuclear metal complexes with large spin ground states is a formidable challenge to synthetic chemists.[8] In strong contrast to the predictive synthetic principles of organic chemistry, it is very difficult to prepare polynuclear metal complexes in a rational manner. In the known polynuclear SMMs, the metal ions are bridged by O^{2-}, OH^-, OR^-, RCO_2, or a combination of two or more of these units. In short, no single strategy is available to prepare a molecule containing, for example, 25 Mn ions. It is also a considerable challenge to systematically build an SMM with an $S = 30$ ground state. Nevertheless, chemists have developed some strategies.

One approach involves a building-block strategy employing small complexes with 2, 3, or 4 metal ions. In this approach, the relatively small building-block complex is treated with a reagent that opens up one side of the complex by removing some of the organic ligands. Silicon forms strong Si–O bonds, so silicon-containing reagents have been employed as RCO_2^- abstraction reagents, and this has often led to aggregation to a polynuclear product with more metal ions. In another approach, polydentate ligands that can form several bonds with one or more metal ions have been added to the building-block complexes to cause aggregation and thus give larger complexes. Using these methodologies, it has been possible to prepare polynuclear Mn complexes with Mn_3, Mn_4, Mn_6, Mn_7, Mn_8, Mn_{10}, Mn_{12}, Mn_{18}, and Mn_{30} compositions.[8]

Unfortunately, bigger is not necessarily better as far as SMMs are concerned. It is important to increase the spin of the ground state, but it is not simply the number of metal ions in the molecule that determines the S value. The pairwise interaction between a Mn^{III} ($S = 2$) ion and a Mn^{IV} ($S = 3/2$) ion can be either antiferromagnetic, pairing up electrons to give a net spin of $S = 1/2$, or ferromagnetic, which would give $S = 7/2$. Magnetic exchange interactions are propagated by the bridging O^{2-}, OH^-, RO^-, or RCO_2^- ligands. Thus, it is necessary to arrange the metal ions and bridging ligands in an appropriate manner so that they give a high spin ground state for the polynuclear complex, (i.e., so that the topology of the complex can be used to obtain a high spin ground state).

A large spin does not by itself, however, ensure that a polynuclear complex will be an SMM with an accessible blocking temperature. For example, Mn^{III}_6 complexes have been prepared with an $S = 12$ ground state, but since the six Mn^{III} ions are arranged in a high-symmetry octahedron, the zero-field splitting is negligible ($D \approx 0$) in these complexes.[9] Similar results have been observed in Mn^{III}_6 rings, where the axes of distortions of the individual ions are oriented parallel to the x, y, and z directions, respectively.[10] These Mn^{III}_6 complexes do not function as SMMs because the barrier depends both on S and D, and D is very small.

Only a few classes of SMMs have been well studied, and the general formulas of these are

- $[Mn_{12}O_{12}(O_2CR)_{16}(H_2O)_4]$,
- $(\text{cation})^+[Mn_{12}O_{12}(O_2CR)_{16}(H_2O)_4]^-$,
- $[Fe_8O_2(OH)_{12}(tacn)_6]Br_8$ (Complex **2**),
- $[Mn_4O_3Cl(O_2CCH_3)_3(dbm)_3]$ (Complex **3**), and
- $[Fe_4(OH)_6(dpm)_3]$ (Complex **4**).

In **2**, the ligand tacn is triazacyclononane; in **3**, dbm^- is the anion of dibenzoylmethane; and in **4**, dpm^- is the dipivaloylmethane anion. In addition to the $[Mn^{IV}_4Mn^{III}_8]$ Complex **1** (R = CH_3), many other $[Mn_{12}O_{12}(O_2CR)_{16}(H_2O)_4]$ SMMs have been characterized in which the substituent R on the carboxylate ligand has been varied extensively.

Chemists can, in many cases, reduce or oxidize a given SMM to change the spin of its ground state. The Mn_{12} complexes with $S = 10$ ground states can be chemically reduced to form salts of the $[Mn_{12}O_{12}(O_2CR)_{16}(H_2O)_4]^-$ anions.[4] These Mn_{12}^- anions have non-integer spin ground states with $S = 19/2$. Non-integer spin nanomagnets have been predicted to have different magnetization tunneling characteristics than an integer spin complex.

The Fe_8 Complex **2** also has an $S = 10$ ground state but has a lower symmetry than **1**, triclinic versus tetragonal.[7] We will see in the following that for this reason, the Fe_8 Complex **2** is better suited to investigating the quantum effects on the dynamics of the magnetization. Unfortunately, it has proven difficult to chemically modify this complex.

The chemistry of SMMs seems ideally suited to examining the effects of changing the spin of a complex from a small value such as $S = 3$ to a large value such as $S = 30$. An $S = 3$ complex is best described by quantum mechanics, whereas an $S = 30$ complex would have a very large number of spin states and could be described by classical mechanics. Is magnetization tunneling seen in both complexes? It was of interest to find that the $[Mn^{IV}Mn^{III}_3]$ Complex **3** has an isolated $S = 9/2$ ground state and functions as an SMM.[11] Chemistry is proving well suited to finding SMMs with spin values that cover a large range.

The chemistry of SMMs provides several other benefits. By changing the ligands on the periphery of a complex, it can be made to be more or less soluble. In this way, it could be possible to prepare thin films of SMMs. In the future, chemistry will be used to attach SMMs to surfaces or polymers. An early effort to make Langmuir–Blodgett films of **1** has been reported.[12] In summary, even though some limitations now exist relative to the capabilities of

chemistry to modify SMMs, it is clear that chemistry will permit a systematic study of the physical phenomena associated with these molecular nanomagnets.

Quantum Tunneling and Quantum Coherence

The magnetization of nano-sized particles can in principle also relax through an under-barrier mechanism via quantum admixing of the "up" and "down" states. Macroscopic quantum tunneling (MQT) has long been sought, following theoretical predictions of its presence in nano-sized magnetic particles.[13] However, MQT must be a rare event, for a macroscopic particle is by definition a system that is large enough to behave classically during most of the time it is being observed. In 1996,[14–16] MQT of the magnetization was first reported for a sample of **1**. In fact, the hysteresis loop, shown in Figure 3, is not smooth. Steps can be observed at regular intervals in the plot of magnetization versus magnetic field. The observed steps in the hysteresis loop correspond to an increase in the rate of change in magnetization occurring when there is an energy coincidence of the levels on the opposite parts of the double-well potential. For these critical field values, tunneling of the magnetization is allowed, and therefore a noticeable increase in the relaxation rate is seen.

The origin of magnetization tunneling in SMMs is still a matter of active research. As illustrated in Figure 4, tunneling occurs between two levels that have the same energy if some admixing of the two states occurs. The transverse interaction that mixes the states and gives rise to the so-called "tunnel splitting" can be provided by low-symmetry components of the crystal field, or by a magnetic field provided either by magnetic nuclei or by the neighboring molecules. The larger the value of m_s, the smaller the admixture of the two wave functions and the lower the tunneling rate. For **1**, no direct evidence of tunneling between the $m_s = \pm 10$ levels has been obtained, while tunneling between smaller m_s levels is indicated by the appearance of steps on the magnetization hysteresis loop (Figure 3).

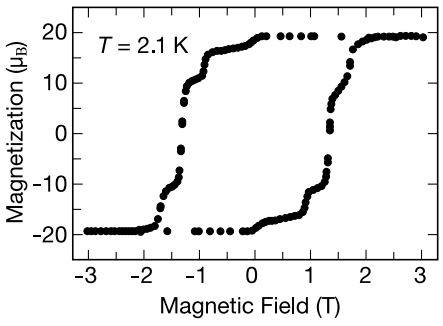

*Figure 3. Magnetization versus magnetic field hysteresis loop for Mn_{12}-acetate Complex **1**. Data were recorded on a single crystal with the magnetic field applied along the tetragonal axis of each Mn_{12} molecule. The vertical parts of the "steps" correspond to critical values of the field where resonant magnetization tunneling is allowed.*

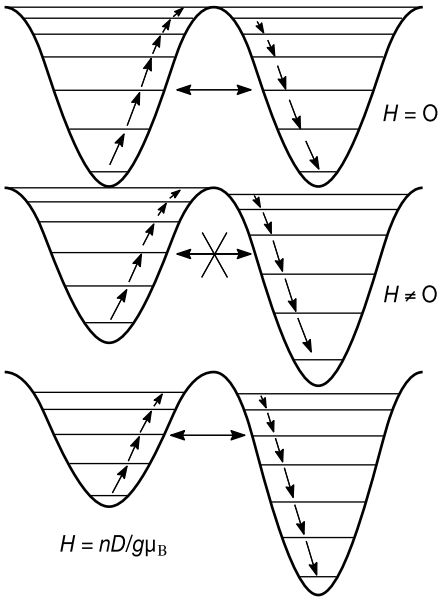

Figure 4. Drawing showing how the potential-energy diagram of an SMM changes as the magnetic field is swept from H = 0 to H = nD/gμ_B. Resonant magnetization tunneling occurs when the energy levels are aligned between the two halves of the diagram.

Detailed studies[7] of the Fe_8 Complex **2** (Figure 5) using HFEPR[17] and inelastic neutron scattering (INS)[18] data clearly indicate that the transverse magnetic anisotropy of the Fe_8 Complex **2** is much larger than that of the Mn_{12} Complex **1**. This means that tunneling between the lowest m_s states can be observed. In fact, the Fe_8 Complex **2** exhibits a temperature-independent magnetization relaxation rate below 0.35 K, which is only explicable in terms of a tunneling of the magnetization occurring in the lowest energy levels, that is, between the $m_s = -10$ and $m_s = +10$ levels.[19] Recently, the very small tunnel splitting in the Fe_8 Complex **2** (i.e., the matrix element that couples the $m_s = -10$ and $m_s = +10$ levels) has been measured.[20] Its dependence on the magnetic field applied along the axis of hard magnetization has also been measured. The application of a field along the hard axis does not necessarily increase the tunneling rate, but gives rise to oscillations, with quenching of the tunneling for critical values of the field where a destructive interference between the tunneling pathways occurs. The tunneling rate oscillates with a period that is simply related to the zero-field splitting parameter(s).[21] By applying a transverse magnetic field, it is therefore possible to control the tunneling rate of the axial magnetization and consequently the coercivity in the hysteresis loops. This phenomenon, which has potential technological applications, is a characteristic feature of SMMs and their intrinsic quantum nature.

In **2**, the tunnel splitting in zero field was found to be of the order of 10^{-8} K. Any axial field that splits the two ground levels by an energy exceeding this value suppresses the tunneling mechanism. In order to rationalize the observation of tunneling, the magnetic field of the nuclei, which is still fluctuating at low temperature, has been considered a source of level broadening and, therefore, of tunneling.

The role of the nuclear magnetic field was very recently definitively established[22] for the Fe_8 Complex **2**. The magnetization relaxation rate of the standard Fe_8 sample was compared with those of two isotopically modified samples: (a) ^{56}Fe replaced by ^{57}Fe and (b) a fraction of the ^{1}H atoms replaced by ^{2}H atoms. The ^{56}Fe atoms had no nuclear spin ($I = 0$), whereas ^{57}Fe had a spin of $I = 1/2$. Similarly, ^{1}H had $I = 1/2$, while ^{2}H had $I = 1$, but with a much smaller gyromagnetic factor. A strong influence of nuclear spins on resonant magnetization tunneling was observed, where the tunneling rate was found to be larger when the hyperfine field was stronger. Manganese-containing SMMs are not suited to this kind of experiment, as the hyperfine field is dominated by the only stable ^{55}Mn isotope ($I = 5/2$).

The interplay of nuclear and electron spins in the dynamics of the macroscopic magnetization seems very appealing for potential use in quantum computing. In fact, the use of the nuclear magnetization through modified nuclear magnetic resonance experiments has been suggested as a model of quantum computing.

The $S = 9/2$ Mn_4 Complex **3** has also been shown to have a temperature-independent magnetization relaxation rate.[11] This complex has a well-isolated $S = 9/2$ ground state with $D = -0.53$ cm^{-1}. Magnetization relaxation rates have been determined in the 0.394–2.00 K range. Below 0.60 K, the rate becomes temperature-

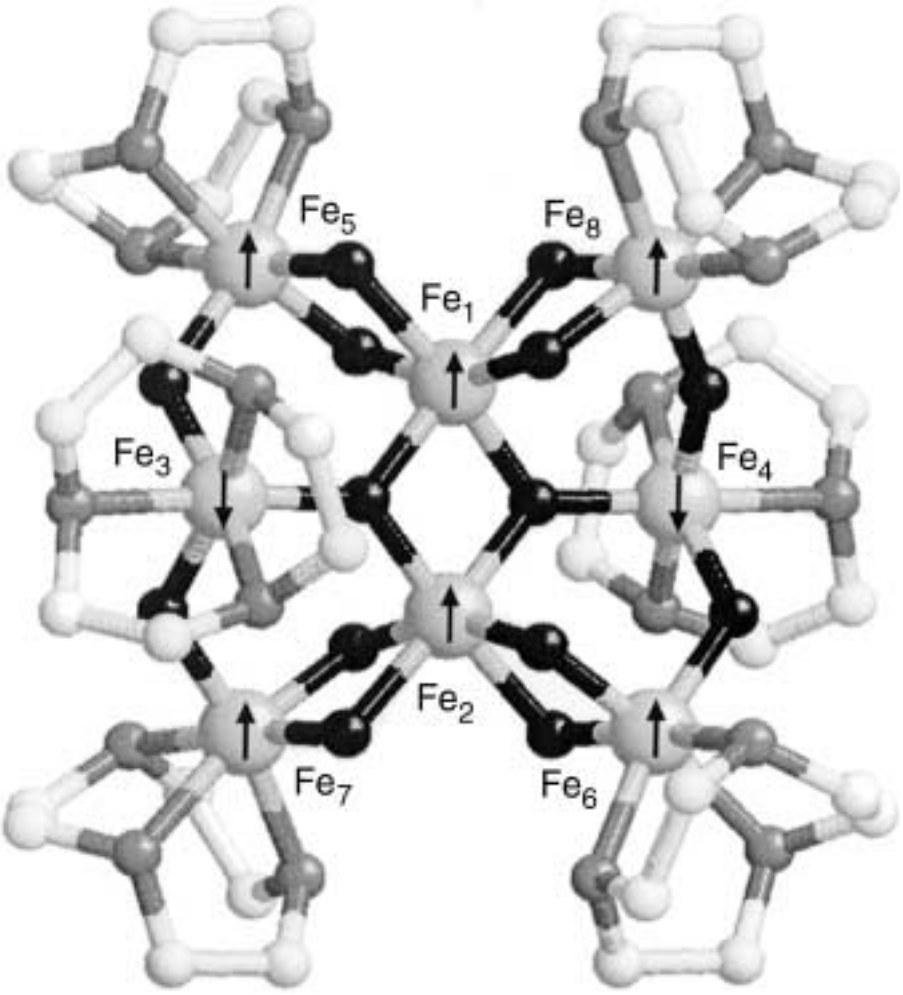

*Figure 5. View of the Fe_8 cluster in Complex **2**. The oxygen atoms are black, nitrogen atoms are dark gray, and carbon atoms are white. The spin structure is represented by the arrows.*

independent, with a rate of 3.2×10^{-2} s^{-1}. Above 0.60 K, the rate is Arrhenius-like, with an activation energy of 11.8 K. This Mn_4 complex shows magnetization tunneling in its $m_s = \pm 9/2$ lowest energy levels. INS data for this complex show the presence of appreciable transverse second-order zero-field interactions, which likely play a crucial role in the tunneling.

Another very significant point to make about the magnetization tunneling for Mn_4 Complex **3** is this: the $m_s = \pm 9/2$ lowest energy levels of this $S = 9/2$ complex comprise a Kramers degenerate pair in *zero magnetic field*. In zero magnetic field, such an $S = 9/2$ molecule cannot coherently tunnel from the $m_s = -9/2$ level to the $m_s = +9/2$ level. However, experimentally a very large step has been seen at zero external magnetic field in the hysteresis loop. It was suggested[11] that in zero external magnetic field, the magnetization tunneling observed for Mn_4 Complex **3** is attributable to a transverse magnetic field due to the nuclear spins of the manganese ions.

The $(cation)^+[Mn_{12}O_{12}(O_2CR)_{16}(H_2O)_4]^-$ salts have $S = 19/2$ SMM anions. As with Mn_4 Complex **3**, this $S = 19/2$ half-integer ground-state SMM should not show magnetization tunneling in zero magnetic field. The salt $(PPh_4)\cdot[Mn_{12}O_{12}(O_2CEt)_{16}(H_2O)_4]$ was first reported in 1995,[23] and the presence of a step occurring at zero external magnetic field was noted two years later.[24] The Kramers degeneracy is removed and tunneling is allowed, even if it is less efficient than in the integer spin analogues, as recently reported.[25]

The power of chemistry to probe exquisite details about how even small changes in the molecular and electronic structures of an SMM affect the rate of magnetization tunneling can be illustrated with the Mn_{12} complex with the *p*-methylbenzoate ligand ($^-O_2CC_6H_4$-*p*-Me). Two crystallographically different forms of the complex have been characterized[26] with the formulas $[Mn_{12}O_{12}(O_2CC_6H_4\text{-}p\text{-}Me)_{16}(H_2O)_4]\cdot(HO_2CC_6H_4\text{-}p\text{-}Me)$ (Complex **5**) and $[Mn_{12}O_{12}(O_2CC_6H_4\text{-}p\text{-}Me)_{16}(H_2O)_4]\cdot 3H_2O$ (Complex **6**). The two Mn_{12} molecules in **5** and **6** are isomers and differ in their arrangements of the H_2O and *p*-methylbenzoate ligands on the peripheries of the complexes. In addition, compared with other Mn_{12} complexes, **5** has an abnormal Jahn–Teller distortion oriented at an oxide ion for one Mn^{III} ion. The cores of these two isomeric complexes are compared in Figure 6. In view of the fact that these two complexes are simply isomers of each other, and very likely have similar ground-state spins and *D* values, the differences in magnetization hysteresis loops (Figure 7) are quite striking. As can be seen, Complex **5**, with the unusual Jahn–Teller distortion at one Mn^{III} ion, has a considerably greater rate of magnetization tunneling than does **6**. The lower crystal site symmetry for the Mn_{12} molecules in **5** leads to greater transverse zero-field interaction and, consequently, an enhanced rate of tunneling.[26]

The presence of two isomers in the same crystal, even if one is present in a much smaller proportion (about 5%), has been observed with micro-SQUID (semiconducting quantum interference device) measurements on a small single crystal of **1**.[27] As the minority phase shows a larger tunneling rate at low temperature, its magnetization can be measured, while that of the majority phase is completely frozen. These recent experiments have evidenced the presence of pure tunneling in the minority phase, as well as the fundamental role played by the manganese hyperfine field.

Future Prospects

Perhaps the most important goal in the field of single-molecule magnets is the preparation of new SMMs with blocking temperatures above liquid-nitrogen temperature, 77 K. This may be achieved by preparing complexes with larger spin ground states that experience appreciable *negative* magnetoanisotropy. Already several compounds with ground spin states larger than 10 have been reported, but their magnetic anisotropy is small and SMM behavior is observed only at temperatures lower than those for the Mn_{12} complexes. It must be emphasized that only the ground state of an SMM can be thermally populated at or below the blocking temperatures. It is clear that complexes with ground states where *S*, for

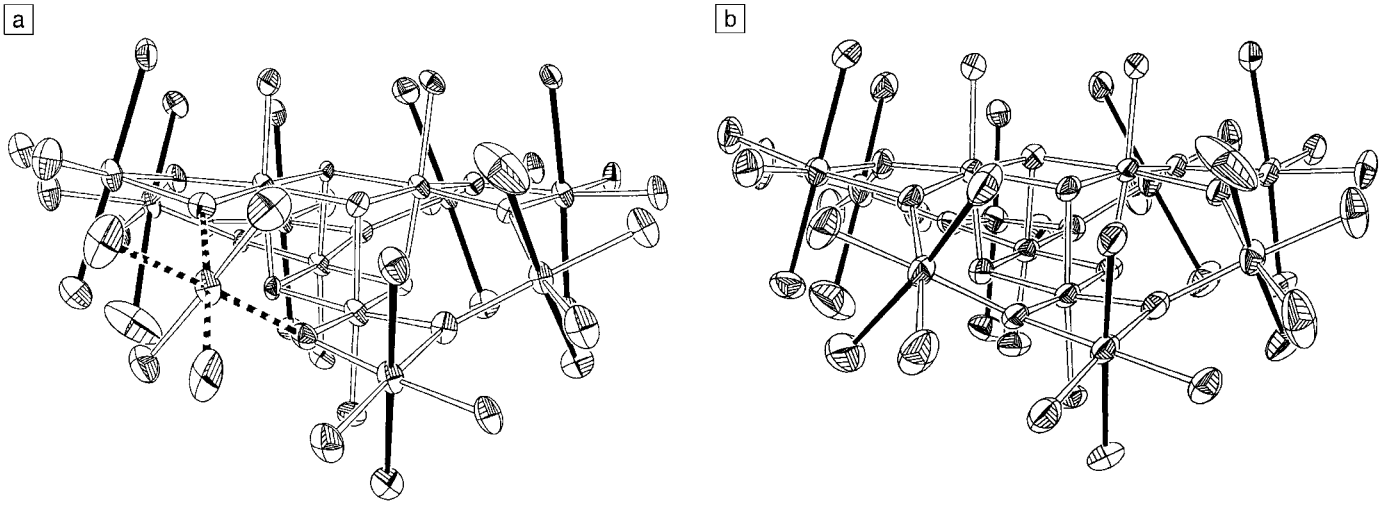

Figure 6. Structures of the cores of the two p*-methylbenzoate Mn_{12} molecules: (a) Complex **5** and (b) Complex **6**. The coordination geometries about each Mn atom are shown. Each of the eight Mn^{III} ions show a tetragonally elongated Jahn–Teller distortion. In the case of **6**, the J–T elongation axes are indicated as solid lines. For **5**, one J–T axis (dashed lines) at one Mn^{III} ion has an unusual orientation pointed at an O^{2-} ion. There are two dashed lines shown because the molecule has a crystallographic C_2 axis disorder.*

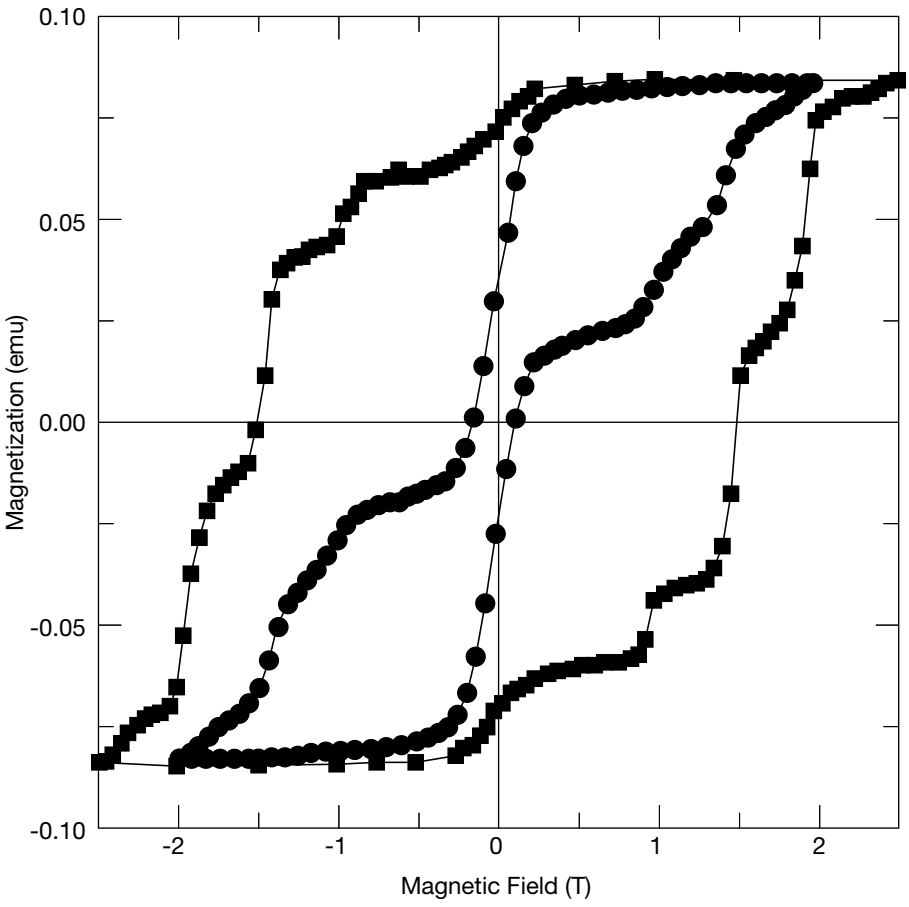

Figure 7. Magnetization hysteresis loops observed for oriented crystals of the p*-methylbenzoate Mn_{12} Complexes **5** (●) and **6** (■) at 1.90 K. The hysteresis loop for **5** has an appreciably smaller coercive field.*

instance, is larger than 30 should be achievable, but it will be challenging to have only the ground state populated at $T = 77$ K.

Another challenge is to make an SMM with a half-integer spin state that has a negligible nuclear spin field. Fe_4 Complex **4** has a ground state with $S = 5$ and shows SMM behavior below 1 K, with pure quantum tunneling of the magnetization below 0.1 K. The one-electron reduction of Fe_4, which has only oxygen atoms in the coordination sphere, seems very promising and is under study. In such a complex, the magnetization tunneling between a pair of $\pm m_s$ levels can be promoted only by the application of an external field, allowing a better control of the hysteresis loop.

Chemistry should lead to the means of attaching SMMs to a variety of substrates. Functionalized metal surfaces could provide some of the ligands to bind SMMs. An ordered array of such SMMs would result. Perhaps functionalized (electrically conductive) polymers could be employed to anchor SMMs. The large magnetoanisotropy of these SMMs could be used to orient the polymers. It is quite clear that it is early in the single-molecule magnetism era.

Acknowledgments

George Christou and David N. Hendrickson thank the National Science Foundation for funding, and all of their very capable collaborators for their contributions. Dante Gatteschi and Roberta Sessoli

thank A. Caneschi, A. Cornia, and W. Wernsdorfer, who have been major contributors to this research. The Italian MURST (Ministero dell'Università e della Ricerca Scientifica e Technologica) is also acknowledged.

References

1. S.M.J. Aubin, M.W. Wemple, D.M. Adams, H.-L. Tsai, G. Christou, and D.N. Hendrickson, *J. Am. Chem. Soc.* **118** (1996) p. 7746.
2. R. Sessoli, H.-L. Tsai, A.R. Schake, S. Wang, J.B. Vincent, K. Folting, D. Gatteschi, G. Christou, and D.N. Hendrickson, *J. Am. Chem. Soc.* **115** (1993) p. 1804.
3. R. Sessoli, D. Gatteschi, A. Caneschi, and M.A. Novak, *Nature* **365** (1993) p. 141.
4. For a list a references on single-molecule magnets, see S.M.J. Aubin, Z. Sun, L. Pardi, J. Krzystek, K. Folting, L.-C. Brunel, A.L. Rheingold, G. Christou, and D.N. Hendrickson, *Inorg. Chem.* **38** (1999) p. 5329.
5. R. Sessoli, *Mol. Cryst. Liq. Cryst.* **274** (1995) p. 145.
6. M.A. Novak, R. Sessoli, A. Caneschi, and D. Gatteschi, *J. Magn. Magn. Mater.* **146** (1995) p. 211.
7. D. Gatteschi, R. Sessoli, and A. Cornia, *Chem. Commun.* (2000) p. 725.
8. G. Aromi, S.M.J. Aubin, M.A. Bolcar, G. Christou, H.J. Eppley, K. Folting, D.N. Hendrickson, J.C. Huffman, R.C. Squire, H.-L. Tsai, S. Wang, and M.W. Wemple, *Polyhedron* **17** (1998) p. 3005.
9. G. Aromi, J.-P. Claude, M.J. Knapp, J.C. Huffman, D.N. Hendrickson, and G. Christou, *J. Am. Chem. Soc.* **120** (1998) p. 2977.
10. G.L. Abbati, A. Cornia, A.C. Fabretti, A. Caneschi, and D. Gatteschi, *Inorg. Chem.* **37** (1998) p. 1430.
11. S.M.J. Aubin, N.R. Dilley, L. Pardi, J. Krzystek, M.W. Wemple, L.-C. Brunel, M.B. Maple, G. Christou, and D.N. Hendrickson, *J. Am. Chem. Soc.* **120** (1998) p. 4991.
12. M. Clemente-León, H. Soyer, E. Coronado, C. Mingotaud, C.J. Gómez-García, and P. Delhaes, *Angew. Chem., Int. Ed. Engl.* **37** (1998) p. 2842.
13. E.M. Chudnovsky and J. Tejada, *Macroscopic Quantum Tunneling of the Magnetic Moment* (Cambridge University Press, Cambridge, 1998).
14. J.R. Friedman, M.P. Sarachik, J. Tejada, J. Maciejewski, and R. Ziolo, *J. Appl. Phys.* **79** (1996) p. 6031.
15. J.R. Friedman, M.P. Sarachik, J. Tejada, J. Maciejewski, and R. Ziolo, *Phys. Rev. Lett.* **76** (1996) p. 3830.
16. L. Thomas, F. Lionti, R. Ballou, D. Gatteschi, R. Sessoli, and B. Barbara, *Nature* **383** (1996) p. 145.
17. A.L. Barra, P. Debrunner, D. Gatteschi, Ch. E. Schulz, and R. Sessoli, *Europhys. Lett.* **35** (1996) p. 133.
18. R. Caciuffo, G. Amoretti, A. Murani, R. Sessoli, A. Caneschi, and D. Gatteschi, *Phys. Rev. Lett.* **81** (1998) p. 4744.
19. C. Sangregorio, T. Ohm, C. Paulsen, R. Sessoli, and D. Gatteschi, *Phys. Rev. Lett.* **78** (1997) p. 4645.
20. W. Wernsdorfer, R. Sessoli, A. Caneschi, D. Gatteschi, A. Cornia, and D. Mailly, *J. Appl. Phys.* **87** (2000) p. 5481.
21. W. Wernsdorfer and R. Sessoli, *Science* **284** (1999) p. 133.
22. W. Wernsdorfer, A. Caneschi, R. Sessoli, D. Gatteschi, A. Cornia, V. Villar, and C. Paulsen, *Phys. Rev. Lett.* **84** (2000) p. 2965.
23. H.J. Eppley, H.-L. Tsai, N. de Vries, K. Folting, G. Christou, and D.N. Hendrickson, *J. Am. Chem. Soc.* **117** (1995) p. 301.
24. S.M.J. Aubin, S. Spagna, H.J. Eppley, K. Folting, G. Christou, and D.N. Hendrickson, *Mol. Cryst. Liq. Cryst.* **305** (1997) p. 181.
25. A.M. Gomes, M.A. Novak, W. Wernsdorfer, R. Sessoli, L. Sorace, and D. Gatteschi, *J. Appl. Phys.* **87** (2000) p. 6004.
26. D. Ruiz, Z. Sun, S.M.J. Aubin, E. Rumberger, C. Incarvito, K. Folting, G. Christou, and D.N. Hendrickson, *Mol. Cryst. Liq. Cryst.* **335** (1999) p. 413.
27. W. Wernsdorfer, R. Sessoli, and D. Gatteschi, *Europhys. Lett.* **47** (1999) p. 254. □